On Information-theoretic limits of Code-domain NOMA for 5G

Article *in* IET Communications · July 2018

DOI: 10.1049/iet-com.2018.5241

CITATIONS
21

READS
829

5 authors, including:

Mai T. P. Le
University of Science and Technology - The University of Danang
18 PUBLICATIONS **106** CITATIONS
SEE PROFILE

Guido Carlo Ferrante
Massachusetts Institute of Technology
28 PUBLICATIONS **136** CITATIONS
SEE PROFILE

Giuseppe Caso
Ericsson
41 PUBLICATIONS **360** CITATIONS
SEE PROFILE

Luca De Nardis
Sapienza University of Rome
123 PUBLICATIONS **1,450** CITATIONS
SEE PROFILE

IET Research Journals

This paper is a postprint of a paper submitted to and accepted for publication in IET Communications and is subject to Institution of Engineering and Technology Copyright. The copy of record is available at the IET Digital Library

IET Journals
The Institution of Engineering and Technology

On Information-theoretic limits of Code-domain NOMA for 5G

ISSN 1751-8644
doi: 0000000000
www.ietdl.org

Mai T. P. Le[1,3] ✉, *Guido Carlo Ferrante*[2], *Giuseppe Caso*[1], *Luca De Nardis*[1], *Maria-Gabriella Di Benedetto*[1]

[1] *Department of Information Engineering, Electronics and Telecommunications, Sapienza University of Rome, Rome 00184, Italy*
[2] *Department of Electrical Engineering, Chalmers University of Technology, Gothenburg 41296, Sweden*
[3] *Faculty of Electronic and Telecommunication Engineering, University of Science and Technology, The University of Da Nang, Da Nang, Vietnam*
✉ *E-mail: mai.le.it@ieee.org*

Abstract: Motivated by recent theoretical challenges for 5G, this paper aims to position relevant results in the literature on code-domain non-orthogonal multiple access (NOMA) from an information-theoretic perspective, given that most of the recent intuition of NOMA relies on another domain, that is, the power domain. Theoretical derivations for several code-domain NOMA schemes are reported and interpreted, adopting a unified framework that focuses on the analysis of the NOMA spreading matrix, in terms of load, sparsity, and regularity features. The comparative analysis shows that it is beneficial to adopt extreme low-dense code-domain NOMA in the large system limit, where the number of resource elements and number of users grow unboundedly while their ratio, called load, is kept constant. Particularly, when optimum receivers are used, the adoption of a *regular* low-dense spreading matrix is beneficial to the system achievable rates, which are higher than those obtained with either *irregular* low-dense or dense formats, for any value of load. For linear receivers, which are more favorable in practice due to lower complexity, the *regular* low-dense NOMA still has better performance in the underloaded regime (load < 1), while the *irregular* counterpart outperforms all the other schemes in the overloaded scenario (load > 1).

1 Introduction

Being acknowledged as an important enabler for 5G multiple access, non-orthogonal multiple access (NOMA) with its diverse dialects recently attracted a huge attention in the wireless community from both industry and academia [1]. In fact, NOMA has been currently proposed by the 3rd Generation Partnership Project (3GPP) for 5G New Radio (NR). Many NOMA schemes for NR were initially proposed in Release-13 (Rel-13) Study Item, and were partly analyzed in Rel-14. While some specifications of 5G-NR have been officially standardized in the current Rel-15 (for example, Specification TS 38.211 for Physical channels and modulation [2]), Specification TS 38.812 for Study on NOMA for NR [2] is still under investigation with the expectation to have a 'ready' NR system in 2020 [3].

In traditional orthogonal multiple access (OMA) schemes, users are allocated to orthogonal resource elements (REs) either in time, frequency, or code domains [4]. Based on the relationship between the number of users K and the number of REs N, also called degrees of freedom, the system is termed *underloaded* when $K < N$ and *overloaded* when $K > N$. As a matter of fact, one should note that underloaded systems can be made OMA under the assumptions of perfect knowledge of channel state information and perfect synchronization between the transmitters and receivers. A very different situation arises when the system is overloaded. Even under ideal conditions such as ideal propagation and ideal allocation strategy, the system is intrinsically affected by 'collisions' due to interference [5]. This scenario may be easily envisioned in 5G, for example in the internet-of-things (IoT), in which a huge number of terminals are required to transmit simultaneously. Noteworthy that, according to this understanding, all conventional OMA schemes, including the well-known CDMA, become NOMA in the overloaded regime, due to the exceedingly large number of users compared to the number of REs.

In order to enable detection at the receiver side, different users are detected based on the difference of power or spreading codes, leading to two main corresponding approaches: power-domain NOMA vs. code-domain NOMA. To address interference provoked by the lack of a sufficient number of REs, controllable interference among REs may be introduced in the code domain with an acceptable complexity of receivers [6]. This NOMA approach is currently known as *code-domain NOMA* [4]. However, with reference to NOMA, most of recent works in the literature focus on the power-domain case [1], which is based on the idea of serving multiple users at the same time/frequency/code with different power levels [1, 4, 7]. This paper, on the other hand, makes an effort to contribute to the understanding of code-domain approach, particularly from an information-theoretic perspective.

Regarding massive connectivity of 5G, the number of users is supposed to be very large compared to the number of REs. The behavior of the system should thus be considered in the asymptotic limit, where both K and N go to infinity, while the ratio $K/N = \beta$, called load, remains finite. This corresponds to analyzing the system in the *large system limit* (LSL) [8]. NOMA schemes and corresponding achievable rates can be investigated in the LSL considering three main features:

- load β, particularly $\beta > 1$, also known as overloading factor, which is considered as a significant feature of code-domain NOMA [4].
- sparsity, describing the structure of code-domain NOMA spreading matrix, whose spreading sequence is commonly designed to be sparse to reduce the detection complexity [4].
- regularity, which characterizes possible spreading mapping constraints [9]. As will be detailed in Sec. 3, *regular* low-dense NOMA refers to the case where the number of users per occupied RE and the number of occupied REs per user are fixed, whereas *irregular* designates the case where these numbers are random and fixed on average [9–11].

The contribution of this paper is twofold. Firstly, it positions relevant information-theoretic results in the literature on code-domain NOMA, by providing a link to previous theoretical analyses of some proposed code-domain NOMA schemes, such as fundamental limits of *irregular* low density-spreading NOMA [12, 13] vs. the *regular* counterpart [10, 11]. This paper addresses a general code-domain NOMA analysis with respect to different cases of sparsity and regularity in both underloaded and overloaded regimes. Secondly, a unified mathematical framework is presented for several code-domain NOMA schemes, from which the corresponding information-theoretic results are expected to explore the relationship between the achievable rates and the aforementioned peculiar features of code-domain NOMA. Understanding the behavior of the

system in terms of information-theoretic bounds can provide crucial insight to select system parameters, and can contribute as a reference for future release of 5G standardization [4].

The rest of the paper is organized as follows: Section 2 introduces the unified analytical framework. The theoretical analysis is presented in Section 3 and obtained results are discussed. Conclusions provided in Section 4 complete the paper.

2 A Unified Framework for Code-domain NOMA

2.1 A reference mathematical model

Some proposed methods for code-domain NOMA include interleave division multiple access (IDMA) [14, 15], low-density spreading CDMA (LDS-CDMA) [16], time-hopping CDMA (TH-CDMA) [12], successive iterative cancellation amenable multiple access (SAMA) [17], multi-user shared access (MUSA) [18], and pattern division multiple access (PDMA) [19, 20], which are all tightly correlated to traditional direct sequence-CDMA (DS-CDMA), as will be shown below. Naturally, the mathematical model may be built from the baseline model of DS-CDMA, proposed by Verdú and Shamai in [8] and [21]. Note that, the above code-domain NOMA techniques are well-matched in the DS-CDMA model, since all are single-carrier systems; other code-domain NOMA schemes, that are proposed for the multi-carrier case, such as low-density spreading OFDM (LDS-OFDM) [22], sparse code multiple access (SCMA) [23], or power domain sparse code multiple access (PSMA), known as a hybrid scheme between power-domain NOMA and SCMA [24], might be properly mapped to multi-carrier models. Some examples can be given as the multi-carrier CDMA in [25], or the multi-carrier NOMA proposed for both power and code-domain NOMA, that focused on other perspectives with respect to spectral efficiency such as user association and resource allocation in [26].

The mathematical model for code-domain NOMA* is described as follows

$$\boldsymbol{y} = \boldsymbol{S}\boldsymbol{H}\boldsymbol{b} + \boldsymbol{n}, \tag{1}$$

where the received signal $\boldsymbol{y} \in \mathbb{C}^N$ belongs to a space characterized by N signal dimensions. Note that N also represents the number of elements over which each symbol is spread, that is the number of REs, and equivalent to the number of 'chips', as termed commonly in CDMA. Vector $\boldsymbol{b} = [b_1, \ldots, b_K]^T \in \mathbb{C}^K$ is the vector of symbols transmitted by K users. Being a random spreading matrix, $\boldsymbol{S} = [\boldsymbol{s}_1, \ldots, \boldsymbol{s}_K] \in \mathbb{C}^{N\times K}$ is composed of K columns, each being the spreading sequence $\mathbf{s}_k$ of user k ($1 \leqslant k \leqslant K$). Supposing the channel is flat, the channel matrix can be represented as $\boldsymbol{H} = \text{diag}\,[h_1, \ldots, h_k] \in \mathbb{C}^{K\times K}$, whereas it reduces to the identity matrix if the AWGN channel is assumed. Lastly, the noise $\boldsymbol{n} \in \mathbb{C}^N$ is described by a circularly-symmetric Gaussian vector with zero mean and covariance $N_0\boldsymbol{I}$.

The nature of the representation matrix $\boldsymbol{S}$ defines the multiple access methods. This matrix is known as spreading matrix or signature matrix in DS-CDMA, TH-CDMA, LDS-CDMA, SAMA, or code matrix in MUSA, and pattern matrix in PDMA. As a matter of fact, NOMA schemes can be classified into dense vs. low-dense, where the corresponding matrix $\boldsymbol{S}$ is dense if all REs are used vs. low-dense, when some REs are not used. In terms of energy, this corresponds to having all REs contain signal energy vs. energy being concentrated on only part of the available REs, reflected by the presence of nonzero entries in $\boldsymbol{S}$. According to this understanding, DS-CDMA inherently stands for dense spreading. The dense group includes DS-CDMA and IDMA, while the low-dense group includes LDS-CDMA, TH-CDMA, SAMA, MUSA, and PDMA. Figure 1 depicts the above NOMA classification, along with an example of $\boldsymbol{S} \in \mathbb{C}^{3\times 4}$ for each scheme†. One should note that to perform fair comparison of systems, energy in the different schemes must be normalized.

2.2 Code-domain NOMA classification

2.2.1 Dense NOMA:

Direct-sequence CDMA (DS-CDMA): In DS-CDMA, spreading codes spread out the energy of signals over all the N available REs [21]. Each column $\boldsymbol{s}_k$ of the representation matrix $\boldsymbol{S}$ is formed by a spreading code sequence, corresponding to a single user k over K users. Two typical examples representing for DS-CDMA spreading codes were described by Verdú and Shamai [21], including binary and spherical sequences. In the binary sequence model, $\boldsymbol{s}_k$ is uniformly filled with N values belonging to the set $\{+1/\sqrt{N}, -1/\sqrt{N}\}$, whereas $\boldsymbol{s}_k$ is modeled as a unitarily invariant unit-norm vector in the spherical model [21]. Matrix $\boldsymbol{S}$ has the dense structure, as illustrated in Fig. 1, for the binary case.

Interleave Division Multiple Access (IDMA): IDMA was shown to be a special case of the traditional CDMA employing a common spreading code and a user-specific random interleaver [14, 15]. In particular, each DS-CDMA spreading code is replaced by a length-N spreading code followed by a chip-interleaver, where the interleavers should be generated independently, randomly, and uniquely for different users [14]. The system model of IDMA can be described comparably to CDMA as follows. In CDMA, the information bit b_k of the user k-th is spread by the corresponding spreading code $\boldsymbol{s}_k$, and the users are separated easily by their respective codes. On the other hand, the user bit b_k of IDMA transmitter is first spread by the *same* spreading code $\boldsymbol{s} = \boldsymbol{s}_k, \forall k$, and then permutated by a user-distinct interleaver π_k. This scheme relies on interleaving process for user separation, thus, is called as interleave division multiple access. The descriptive transmitter model of IDMA is presented in comparison with that of CDMA in Fig. 2.

By sharing a single spreading code for all users, the receiver complexity of IDMA was shown to be lower than CDMA, while higher spectral efficiency can be achieved [14, 15]. With optimal power allocation, the IDMA system capacity may reach to the maximum capacity of the multiple access CDMA for binary AWGN channel, given the same input constraints [14]. By adopting the similar strategy of separating users, the representation matrix $\boldsymbol{S}$ can be identically illustrated in both DS-CDMA and IDMA (see Fig.1).

2.2.2 Low-dense NOMA:

Low-Density Spreading CDMA (LDS-CDMA) and Time-Hopping CDMA (TH-CDMA): LDS-CDMA replaces dense spreading sequences of DS-CDMA by sparse counterparts, as such the dense matrix $\boldsymbol{S}$ in DS-CDMA becomes sparse in LDS case [16]. Consequently, the energy of LDS-CDMA signals concentrates on a part of the REs, in lieu of uniformly spreading over all REs, as in DS-CDMA. The idea on exploiting the sparsity of multiple access based on code domain came from sparse CDMA, which was firstly investigated via statistical physics in [27] and [28], and subsequently studied in [9, 29].

It is worthy to note that, the same sparse structure can be observed in the time-hopping CDMA model [12], hence, both can be depicted by a matrix $\boldsymbol{S}$, composed by N REs with only $N_s \ll N$ nonzero elements in the set $\{+1/\sqrt{N_s}, -1/\sqrt{N_s}\}$, while the remaining $(N - N_s)$ REs are zeros (see Fig. 1*).

Successive Iterative Cancellation Amenable Multiple Access (SAMA): SAMA is a special case of LDS-CDMA [17]. Here, K is fixed to $K = 2^N - 1$, that is, the system is necessarily overloaded. Again matrix $\boldsymbol{S}$ contains '0' and '1' elements, with a specific

*Code-domain NOMA is called shortly as NOMA afterwards.

†*Excluding the SAMA matrix* $\boldsymbol{S} \in \mathbb{C}^{2\times 3}$ *due to its specific constraint as described in* 2.2.2.

**In Fig.1, LDS-CDMA also stands for TH-CDMA*

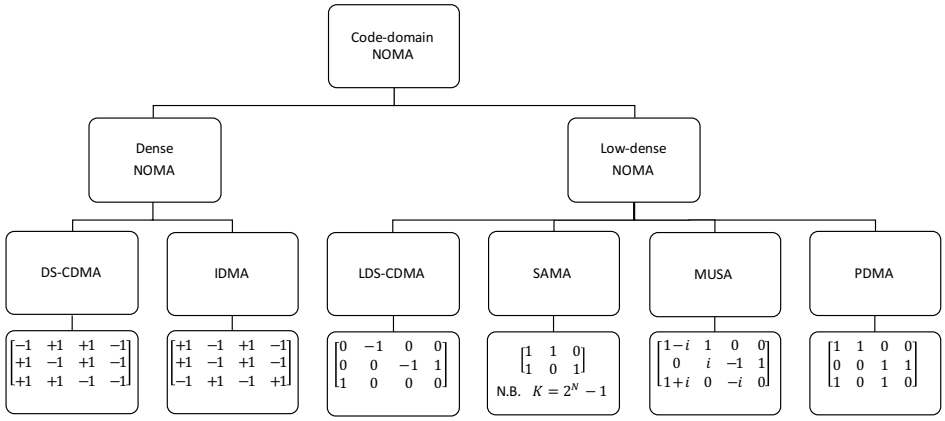

Fig. 1: Code-domain NOMA classification and a corresponding example of matrix for each NOMA dialect

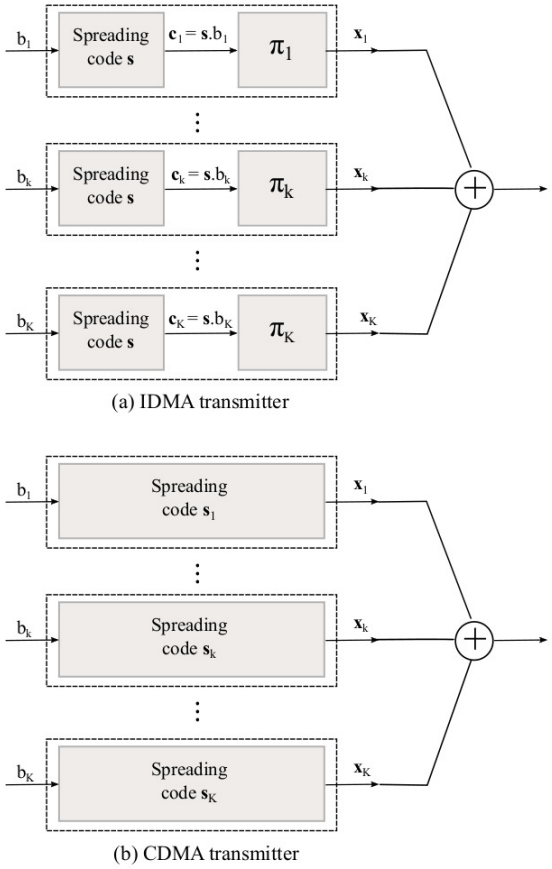

(a) IDMA transmitter

(b) CDMA transmitter

Fig. 2: IDMA vs. CDMA transmitter

structure designed to be effective in the successive inteference cancellation (SIC) based detector [17]. An example of SAMA matrix $\boldsymbol{S} \in \mathbb{R}^{2\times 3}$ is provided in Fig. 1, due to the specific constraint on the ratio K/N. With such peculiar design, SAMA was demonstrated to achieve better performance in terms of bit error rate, compared to the orthogonal counterpart [17].

Multi User Shared Access (MUSA): Along with overloading, grant-free access is another key feature of MUSA [18]. This strategy allows each user to choose its spreading sequence freely from a large cardinality, that, in fact, omits the need for resource coordination by the base station. By adopting grant-free access, MUSA can reduce signaling overhead and transmission delay caused by conventional grant-based transmission. In this way, MUSA lowers power consumption of devices, and thus is proposed for the uplink transmission [18]. MUSA spreading sequences are required to have short length and low cross-correlation to support a large number of grant-free access users and minimize the impact of user collision. It is, in general, difficult to design a large number of binary spreading codes with low correlation. Non-binary and complex-value random spreading codes with M-ary values were proposed for MUSA to address this drawback. Two typical examples of available sets, before normalization, are $\{1+i, -1+i, -1-i, 1-i\}$ ($M = 2$) and $\{0, 1, 1+i, i, -1+i, -1, -1-i, -i, 1-i\}$ ($M = 3$). The entries of these sets are taken from complex spreading codes in the respective M-ary set, as shown in Fig. 3 for the two respective sets $M = 2$ (a) and $M = 3$ (b). A MUSA matrix example for $M = 3$ is shown in Fig. 1.

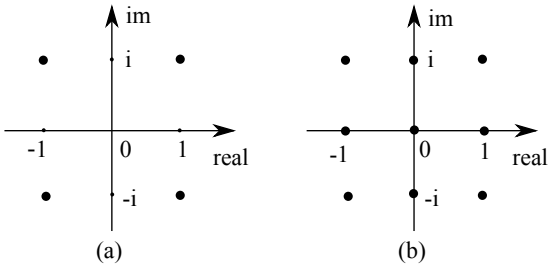

Fig. 3: Examples of MUSA entries: (a) $M = 2$, (b) $M = 3$

Pattern Division Multiple Access (PDMA): The feature that identifies a NOMA scheme as PDMA is the presence of non-orthogonal patterns in place of spreading sequences in LDS-CDMA [19]. PDMA patterns are used to map the transmitted data to a resource group, that can be time, frequency, spatial resource or any combination of those resources. The concept of PDMA patterns could be understood in a broader way compared to spreading codes. Elements of a PDMA pattern matrix can be either filled with binary numbers in the general case, or additionally weighted by power scaling and phase shifting in the extended case. Accordingly, the patterns of PDMA assigned to each user admit the following description

$$s_k = \begin{cases} \{0, 1\} & \text{in the general case} \\ \{0, \alpha_{ki} e^{-j\phi_{ki}}\} & \text{in the extended case,} \end{cases}$$

where α_{ki} and ϕ_{ki} denote power scaling and phase shifting of the k^{th} user on the i^{th} RE, respectively.

The pattern is designed to enable user separation so that every user has its respective pattern, and as such more users can be multiplexed on a limited number of REs, i.e. is intrisically realized as an overloaded system. In addition, to reduce the receiver complexity, sparsity is also introduced in PDMA patterns. In this way, PDMA is characterized by overloading and sparsity features, and is thus realized as a low-dense code-domain NOMA scheme. For example, six users with their different patterns can be mapped to three REs, where one user data can be mapped to one, or even all three REs [19]. An example of the PDMA pattern matrix for $N = 3,\ K = 6$ is

$$\boldsymbol{S}_{\text{PDMA}} = \begin{bmatrix} 1 & 1 & 0 & 1 & 0 & 0 \\ 1 & 0 & 1 & 0 & 1 & 0 \\ 0 & 1 & 1 & 0 & 0 & 1 \end{bmatrix}.$$

With the flat fading assumption, the channel matrix is given as $\boldsymbol{H} = \text{diag}\,[h_1, \ldots, h_6]$. The received signal is achieved as

$$\begin{bmatrix} y_1 \\ y_2 \\ y_3 \end{bmatrix} = \begin{bmatrix} h_1 & h_2 & 0 & h_4 & 0 & 0 \\ h_1 & 0 & h_3 & 0 & h_5 & 0 \\ 0 & h_2 & h_3 & 0 & 0 & h_6 \end{bmatrix} \begin{bmatrix} b_1 \\ b_2 \\ b_3 \\ b_4 \\ b_5 \\ b_6 \end{bmatrix} + \begin{bmatrix} n_1 \\ n_2 \\ n_3 \end{bmatrix}. \qquad (2)$$

By optimizing power scaling and phase shifting factors in the pattern matrix, PDMA scheme can significantly improve spectral efficiency compared with OMA techniques [19, 20]. The PDMA representation matrix provided in the Fig.1 stands for the general case.

A summary of aforementioned low-dense NOMA schemes is provided in the Appendix, where they are shown to have a mutual link. Particularly, SAMA, MUSA, and PDMA are shown to be well connected with LDS-CDMA, which all are reflected by sparsity nature of the matrix $\boldsymbol{S}$. It is reasonable then to take LDS-CDMA as a representative for low-dense NOMA to compare with the dense case from the information-theoretic viewpoint.

3 Theoretical analysis of Code-domain NOMA

In this section, the theoretical behavior of NOMA is analyzed under the impact of three main factors, that are: load, sparsity and regularity. First, the load factor provides a straightforward way to study the system behavior in the underloaded ($\beta < 1$) vs. overloaded ($\beta > 1$) regimes. As mentioned above, overloaded systems are necessarily NOMA, since as soon as β overcomes the boundary value $\beta = 1$, new users find all REs occupied. In fact, all NOMA schemes introduced in Section 2 are characterized by overloaded property, i.e. $\beta > 1$.

The second typical feature under analysis is the dense vs. low-dense aspect, corresponding to the dense vs. low-dense groups as in Fig. 1. Either all N dimensions are used, as in CDMA or IDMA, or only a part of the dimensions is used, as in low-dense systems. Due to sparsity, the system can be graded from dense to extreme low-dense. The number of used dimensions, that we call N_s, defines the *degree of sparseness*. If $N_s = N$, the system is dense. If $N_s = 1$, then the system is extreme low-dense. All other degrees of sparseness lie in between these two extreme cases. The dense vs. low-dense feature is directly reflected by the properties of matrix $\boldsymbol{S}$, as defined in the mathematical model (eq. (1)). Regarding the energy feature, the matrix $\boldsymbol{S}$ of low-dense system contains most of elements that are '0', where '0' indicates elements with zero energy. A heuristic way to think of NOMA scheme is thus as a version of the overloaded CDMA scheme and low-dense NOMA can be referred to as sparse overloaded CDMA [27]. Naturally, it is expected to investigate the effect of those NOMA parameters, including the load β and the degree of sparseness N_s, on theoretical behavior of dense vs. low-dense NOMA.

Achievable rates of low-dense NOMA in the LSL were early and extensively evaluated via sparse CDMA by means of the replica method, also known as heuristic statistical physics, in [9, 27–29].

Table 1 Summary of available theoretical bounds with corresponding references in the literature

	Dense NOMA	Low-dense NOMA			
	($N_s = N$)	($1 < N_s < N$)		($N_s = 1$)	
		Irregular	Regular	Irregular	Regular
Optimum receivers	Eq. (4) [21]	Eq. (3) by Monte-Carlo simulations [21]	Eq. (11) [11]	Eq. (6) [12]	Eq. (13) of this paper
Linear receivers	Eqs. (7, 8) [21]	Eq. (9) [12]	Eq. (14) [11]	Eq. (10) [12]	Eq. (15) of this paper

Since the derivations provided by replica method were typically non-rigorous, the information-theoretic analyses on low-dense NOMA were found rigorously via closed-form expressions in LDS/TH-CDMA model [12, 13], and in regular sparse NOMA model [10, 11]. Given that multiple system models are possibly proposed due to different assumptions, below we reported all curves along with the existing relevant theoretical results in our unified model (c.f. 2.1).

Regarding the third feature, the regularity, low-dense NOMA ($N_s < N$) are further classified into *irregular* vs. *regular* based on spreading mapping constraints, given that N_s is also the number of *occupied* REs per user, whereas N is the total number of REs per user. Previous works on sparse CDMA and low-dense NOMA were classified as *irregular* since the number of occupied REs per user was randomly Poissonian distributed with fixed mean [27, 28], and randomly uniformly distributed [12, 13]*, respectively. On the other hand, in terms of spreading matrix, the regularity assumption in [10, 11] requires matrix $\boldsymbol{S}$ be structured with exactly $N_s \in \mathbb{N}^+$ and $\beta N_s \in \mathbb{N}^+$ non-zero entries per column and row, respectively. It is equivalent to have each user occupying N_s REs and each RE being allocated with exact βN_s users, subject to N_s and βN_s being integers. It is, in general, challenging to have such an ideal model in practical scenarios where users are not allowed to independently select the spreading sequences, they must be coordinated or central scheduled [10]. The *regular* low-dense NOMA via *regular* sparse CDMA was early demonstrated to be superior to the dense in terms of bit error rate in high noise regime in [9], and in terms of spectral efficiency via explicit analytical expressions in recent works [10, 11].

In the following, theoretical behavior of *irregular* vs. *regular* low-dense NOMA ($N_s < N$) is analyzed with the adopted reference models LDS/TH-CDMA [12, 13] vs. regular sparse NOMA [10, 11], respectively. DS-CDMA is adopted as a representative of the dense NOMA group ($N_s = N$) [21]. Both optimal and linear receivers are considered in all cases. Spectral efficiency expressions [bits/s/Hz] for different cases are reported for the self-contained purpose of the paper. It is important to notice that the theoretical results of *irregular* low-dense NOMA are available only for $N_s = 1$ [12, 13] (see 3.1), while closed-form expressions of the *regular* case are valid only for intermediate degrees of sparseness, specifically for $N_s \geqslant 2, \beta N_s \in \mathbb{N}^+$ [11] (see 3.2). For *irregular* low-dense NOMA, since the closed-form expressions for intermediate N_s do not exist yet in the literature (and in general, are not easy to achieve), the results will be shown via Monte Carlo simulations for a full coherent overview. For *regular* low-dense NOMA, the regularity in case of $N_s = 1$ yields a typical setting, which includes a set of parallel Gaussian multiple access channels (MAC), that will be investigated further in 3.2. The references for mapping information-theoretic results in code-domain NOMA are summarized in Table 1, with the corresponding numbered equations in this paper.

3.1 Dense vs. Irregular low-dense NOMA

In this part, theoretical behavior of dense vs. *irregular* low-dense NOMA is analyzed with the two corresponding reference models, that are DS-CDMA ($N_s = N$) [21] and LDS/TH-CDMA ($N_s < N$)

The irregular low-dense NOMA in [12, 13] is called as partly-regular sparse NOMA in [10, 11].

[12]. Since the AWGN channel is used for both cases, the channel matrix $\boldsymbol{H}$ in eq. (1) becomes an identity matrix. The *only difference* in the mathematical model between DS-CDMA and LDS-CDMA is situated in the sparseness of matrix $\boldsymbol{S}$. In DS-CDMA ($N_s = N$), all entries of $\boldsymbol{S}$ are randomly filled by binary values of $\{\pm 1\}$, while in LDS-CDMA, for example with $N_s = 1$, each column of $\boldsymbol{S}$, representing a user, contains only *one* nonzero entry ($\{+1\}$ or $\{-1\}$), and all the rest are nil.

3.1.1 Optimum receivers: The general spectral efficiency for optimum receivers in both dense NOMA and low-dense NOMA cases can be computed via [11, 12, 21]

$$C_{\text{opt}}^{N}(\gamma) = \frac{1}{N} \log_2 \det[\boldsymbol{I} + \gamma \boldsymbol{S}\boldsymbol{S}^*], \tag{3}$$

where γ denotes the signal-to-noise (SNR) ratio.

Dense NOMA: The optimum capacity for the dense case is equal to [21]

$$\begin{aligned} C_{\text{opt}}^{\text{dense}}(\beta, \gamma) = &\frac{\beta}{2} \log_2 \left(1 + \gamma - \frac{1}{4}\mathcal{F}(\gamma, \beta)\right) \\ &+ \frac{1}{2} \log_2 \left(1 + \gamma\beta - \frac{1}{4}\mathcal{F}(\gamma, \beta)\right) \\ &- \frac{\log_2 e}{8\gamma}\mathcal{F}(\gamma, \beta), \end{aligned} \tag{4}$$

where

$$\mathcal{F}(x, z) \coloneqq \left(\sqrt{x(1+\sqrt{z})^2 + 1} - \sqrt{x(1-\sqrt{z})^2 + 1}\right). \tag{5}$$

Irregular low-dense NOMA:

- $1 < N_s < N$: In order to study the behavior of the system, Monte-Carlo simulations are introduced for optimum receivers of *irregular* low-dense NOMA based on eq. (3).
- $N_s = 1$: The closed-form capacity expression of the *irregular* case is [12]

$$C_{\text{opt}}^{\text{irreg}}(\beta, \gamma) = \sum_{k \geqslant 0} \frac{\beta^k e^{-\beta}}{k!} \log_2 (1 + k\gamma). \tag{6}$$

It is worth mentioning that, Maximum Likelihood is typically adopted as the optimum receiver and is, in general, favorably replaced in real-world communication systems by sub-optimal receivers due to complexity issue.

3.1.2 Linear receivers: For dense NOMA, closed-form capacity expressions for all linear receivers are available as in [21]. For *irregular* low-dense NOMA, while the same mutual information is obtained for different linear receivers, including minimum mean square error (MMSE), single user matched filter (SUMF), and zero forcing (ZF) with respect to the particular case $N_s = 1$, closed-form achievable rates for $1 < N_s < N$ are available only for the SUMF receiver [12]).

Dense NOMA: The spectral efficiency of SUMF and MMSE receivers for the dense system in the LSL is [21]

$$C_{\text{SUMF}}^{\text{dense}}(\beta, \gamma) = \frac{\beta}{2} \log_2 \left(1 + \frac{\gamma}{1 + \gamma\beta}\right), \tag{7}$$

and

$$C_{\text{MMSE}}^{\text{dense}}(\beta, \gamma) = \frac{\beta}{2} \log_2 \left(1 + \gamma - \frac{1}{4}\mathcal{F}(\gamma, \beta)\right), \tag{8}$$

where $\mathcal{F}(\gamma, \beta)$ is defined as in eq. (5).

Irregular low-dense NOMA: Due to the peculiar sparse structure of matrix $\boldsymbol{S}$ in LDS-CDMA when $N_s = 1$, the linear receivers (MMSE, SUMF, ZF) yield the same mutual information, while it remains unknown for the in-between cases $1 < N_s < N$ for the MMSE and ZF receivers [12]. Therefore, theoretical behavior of *irregular* low-dense NOMA linear receivers for the intermediate degree of sparseness cases is investigated via the mutual information of the SUMF receiver of LDS-CDMA [12] as follows:

- $1 < N_s < N$: The mutual information of *irregular* low-dense NOMA with the SUMF receiver writes [12]

$$R_{\text{lin}}^{\text{irreg}}(\beta, \gamma, N_s) = \beta \sum_{k \geqslant 0} \frac{(N_s^2\beta)^k}{k!} e^{-N_s^2\beta} \log_2 \left(1 + \frac{\gamma}{1 + \frac{k}{N_s}\gamma}\right). \tag{9}$$

- $N_s = 1$: The closed-form expression of the *irregular* low-dense achievable rate with linear receivers when $N_s = 1$ is [12]

$$R_{\text{lin}}^{\text{irreg}}(\beta, \gamma) = \beta \sum_{k \geqslant 0} \frac{\beta^k e^{-\beta}}{k!} \log_2 \left(1 + \frac{\gamma}{k\gamma + 1}\right). \tag{10}$$

Figure 4 shows the achievable rates of dense vs. *irregular* low-dense systems with optimum and linear receivers as a function of β with fixed value of $E_b/N_0 = 10$ [dB]. With respect to load factor β, the border line (vertical dashed line) at $\beta = 1$ divides Fig. 4 into two areas corresponding to OMA (underloaded with $\beta < 1$) and NOMA (overloaded with $\beta > 1$), with dark and light shaded area, respectively.

In the LSL, Fig. 4 shows that for optimum receivers, dense systems always outperform *irregular* low-dense, irrespective of β, that is, whether OMA or NOMA. Achievable rates for the *irregular* type drop with N_s from the dense case ($N_s = N$) to the extreme low-dense case ($N_s = 1$), and the gap between the *irregular* low-dense and dense becomes negligible at $N_s = 2$, and tends to vanish from $N_s > 2$, e.g. $N_s = 5$. On the other hand, the behavior of linear detection changes, with respect to the level of density of the system. For MMSE receivers, achievable rates of the dense systems are higher than the *irregular* low-dense in the OMA area, while this situation is inverse in the NOMA area, starting from about $\beta > 1.2$. With growing N_s, for example $N_s = \{2, 5\}$, the gap between the achievable rates of *irregular* low-dense NOMA with the SUMF receiver and dense NOMA, sharply reduces, to converge to the SUMF dense curve. Given that optimum detection is unfeasible to implement in practice due to the receiver complexity, the above observation provides the ground for suggesting *irregular* low-dense NOMA in the LSL, for example, for *irregular* low-dense case with $N_s = 1$.

The reported analysis holds in the case of flat-fading channel, as investigated and proved in [13].

3.2 Dense vs. Regular low-dense NOMA

Theoretical analysis of *regular* low-dense NOMA is investigated in this part, in comparison with the dense case.

- $1 < N_s < N$: Closed-form expressions of *regular* low-dense NOMA achievable rates for both optimum and MMSE receivers in [11] are valid under the following constraints:
  - if each user has $2 \leq N_s \in \mathbb{N}^+$ non-zero entries in its spreading sequence, $2 \leq \beta N_s \in \mathbb{N}^+$ users shoud be assigned in the same RE;
  - spreading matrix $\boldsymbol{S}$ is assumed to converge to a bipartite Galton-Watson tree in the LSL (see ([11], Theorem 2) for a full description).

To effectively induce non integer values of N_s and βN_s, one may employ time-sharing between different $(N_s, \beta N_s)$ points in the admissible set to achieve the same total throughput as mentioned in ([11], Remark 4).

- $N_s = 1$: The regularity imposes $\beta \in \mathbb{N}^+$ users per each RE, that is equivalent to having a set of N parallel Gaussian MAC channels [30]. This observation may bring more insight on the behavior of the *regular* with respect to optimum and linear receivers.

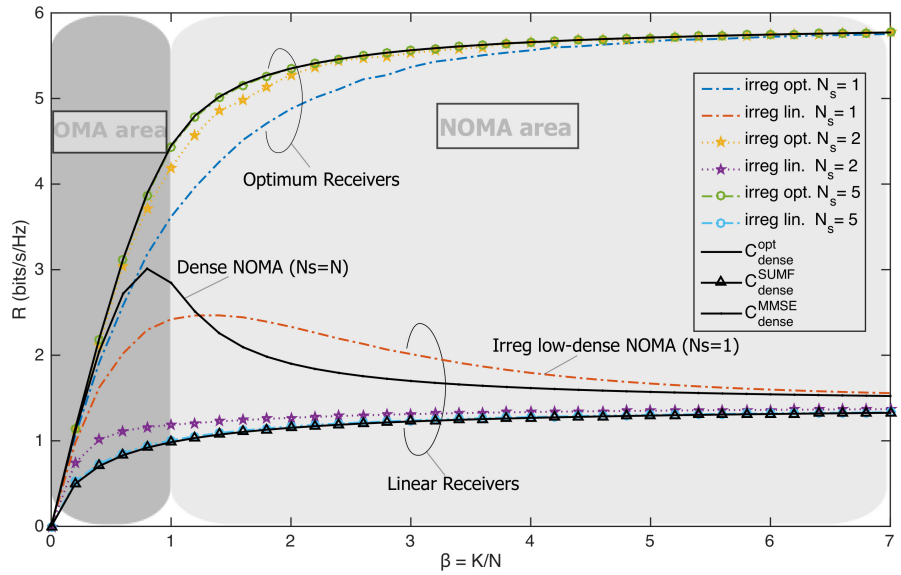

Fig. 4: Achievable rates (bits/s/Hz) of dense NOMA vs. *irregular* low-dense NOMA as a function of β with fixed $E_b/N_0 = 10$ [dB] (parts of the data used to draw this figure were extracted from [12])

$$\mathcal{G}(x,y,z) \coloneqq \left(\frac{\sqrt{(y-(1-\sqrt{z})^2)(x(1+\sqrt{z})^2+1)} - \sqrt{(y-(1+\sqrt{z})^2)(x(1-\sqrt{z})^2+1)}}{\sqrt{y-(1-\sqrt{z})^2} - \sqrt{y-(1+\sqrt{z})^2}} \right)^2, x,y,z \in \mathbb{R}^+, y \geqslant (1+\sqrt{z})^2. \tag{12}$$

3.2.1 *Optimum receivers:*

- $1 < N_s < N$: For the *regular* one, the closed-form expression of optimum capacity is valid for $N_s \geqslant 2$, subject to $N_s, \beta N_s$ being integers [11]

$$\begin{aligned} C^{\text{reg}}_{\text{opt}}(\gamma,\beta,N_s) = {} & \frac{\beta(N_s-1)+1}{2}\log_2\left(1+(\delta+\alpha)\gamma-\frac{1}{4}\mathcal{F}(\delta\gamma,\tilde{\beta})\right) \\ & + (\beta-1)\log_2\left(1+\alpha\gamma-\frac{1}{4}\mathcal{F}(\delta\gamma,\tilde{\beta})\right) \\ & - \frac{\beta(N_s-1)-1}{2}\log_2\left(\frac{(1+\beta N_s\gamma)^2}{\mathcal{G}(\delta\gamma,\psi,\tilde{\beta})}\right), \end{aligned} \tag{11}$$

where $\alpha \coloneqq 1-1/N_s$, $\delta \coloneqq \beta - 1/N_s$, $\tilde{\beta} \coloneqq \alpha/\delta$, $\psi \coloneqq \beta N_s/\delta$, $\mathcal{F}(x,z)$ defined in (5) and $\mathcal{G}(x,y,z)$ defined as in eq. (12) below.

- $N_s = 1$: In this case, the *regular* low-dense NOMA scheme turns out a set of N parallel Gaussian MAC channels, each with β ($1 < \beta \in \mathbb{N}$) users. This setting makes sense only in the overloaded regime. One may easily obtain the spectral efficiency that in this case is

$$C^{\text{MAC}}_{\text{opt}}(\beta,\gamma) = \log_2(1+\beta\gamma). \tag{13}$$

It is worth highlighting that finding the spectral efficiency as a function of E_b/N_0 (via the relation $E_b/N_0 = \beta\gamma/C(\gamma)$ [8]) yields exactly the Cover-Wyner bound as in [21], corresponding to a system with no spreading.

The behavior of *regular* low-dense NOMA vs. dense NOMA with optimum receivers is shown on Fig. 5. For the sake of full comparison, theoretical behavior of the *irregular* low-dense with $N_s = 1$ and the orthogonal case are also plotted for reference. Achievable rates are plotted as a function of system load β, for a fixed value of $E_b/N_0 = 10$ [dB] (Fig. 5a), and as a function of E_b/N_0, for fixed $\beta = 2$ (Fig. 5b). In contrast to the *irregular* counterpart, achievable rates for the *regular* low-dense NOMA, which are superior to all other cases, grow gradually for lower values of $N_s < N$, and reach the ultimate rate (Cover-Wyner bound) when $N_s = 1$.
The reason that makes the optimal spectral efficiency of the *irregular* low-dense to be lower than the dense case may be caused by the random nature of user-resource allocation, leading to a condition in which some users are not assigned with any RE, while some REs are left unused. On the other hand, the regularity feature of the *regular* low-dense NOMA contributes to increasing the optimal spectral efficiency by employing user-mapping intentionally. Nonetheless, this also imposes as a direct consequence additional practical challenges in having some kind of coordination while allocating the resources to users [10, 11].

3.2.2 *Linear receivers:*

- $1 < N_s < N$: The closed-form expressions of *regular* low-dense NOMA achievable rates for linear MMSE (LMMSE) are [11]

$$C^{\text{reg}}_{\text{LMMSE}}(\gamma,\beta,N_s) = \beta\log_2\left(\frac{1+\beta N_s\gamma}{1+N_s\delta\gamma-\frac{N_s\mathcal{F}(\delta\gamma,\tilde{\beta})}{4}}\right), \tag{14}$$

where δ, $\tilde{\beta}$, $\mathcal{F}(x,z)$ defined as in eq. (11).

- $N_s = 1$: In this particular case, the achievable rate of the *regular* low-dense NOMA with respect to the LMMSE receiver may be derived via the setting of parallel MAC channels, each with β users as follows

$$R^{\text{MAC}}_{\text{LMMSE}}(\gamma,\beta) = \beta\log_2\left(1+\frac{\gamma}{1+(\beta-1)\gamma}\right). \tag{15}$$

Figure 6 shows the achievable rates of MMSE, ZF, SUMF receivers for the dense ($N_s = N$), LMMSE receiver for the *regular* low-dense schemes with $N_s = \{1,2,5\}$. The linear receiver for the *irregular* low-dense NOMA with the typical case $N_s = 1$ is also shown for comparison. A remarkable observation from low-dense NOMA with $N_s = 1$ can be given: capacity of *regular* low-dense NOMA with linear receiver outperforms all the rest when $\beta \leqslant 1$ (OMA area), particularly to the typical setting when $N_s = 1$; while in the overloaded regime (NOMA area), there is an intersection where capacity of *irregular* low-dense NOMA with $N_s = 1$ outperforms all other cases. By numerical equation solving, the exact value of the intersection is located at $\beta = 1.232$, from which *irregular* low-dense

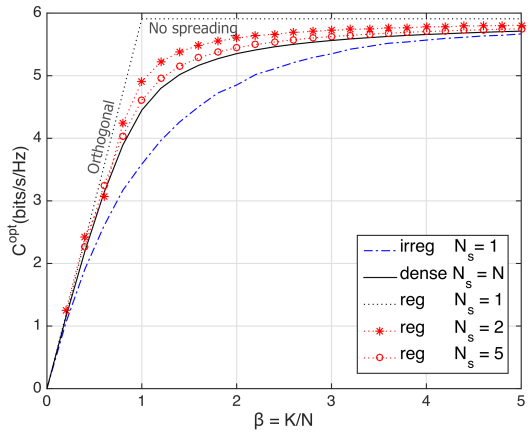

(a)

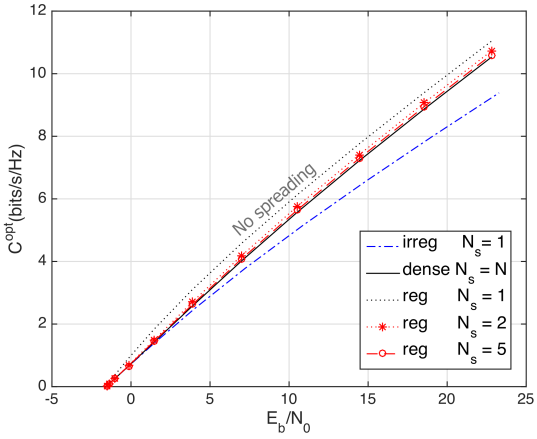

(b)

Fig. 5: Achievable rates (bits/s/Hz) of dense NOMA ($N_s = N$) vs. *regular* and *irregular* low-dense NOMA ($N_s < N$) with optimum receivers
(a) as a function of $\beta = K/N$ for fixed $E_b/N_0 = 10$ [dB]
(b) as a function of E_b/N_0 for fixed $\beta = 2$

NOMA with $N_s = 1$ dominates those of dense NOMA (c.f. Figs. 4 and 5), as well as with all other degrees of sparseness ($N_s > 1$) till about $\beta \approx 5$, and then tend to converge for $\beta > 5$ (with the negligible gap of about 5% at $\beta = 5$). These observed results can be used as a driving rationale in system design.

4 Conclusion

Motivated by the key challenge of finding and analyzing theoretical bounds for NOMA in massive communications, this paper sheds some light on the relationship between achievable rates and NOMA parameters, such as load factor, degree of sparseness and regularity. A unified framework for several code-domain NOMA schemes was presented. The analytical framework, built on the traditional DS-CDMA model, proved to be flexible enough for representing several code-domain dialects, and, in particular, addressed properties of a fundamental element of the model, that is, the representation matrix $\boldsymbol{S}$.

Theoretical investigations were interpreted in the LSL for both optimum and linear receivers, based on closed-form expressions existing for three distinctive cases, that are, dense vs. *regular* low-dense and *irregular* low-dense NOMA, corresponding to DS-CDMA ($N_s = N$) [21] vs. LDS-CDMA ($N_s = 1$) [12] and *regular* sparse

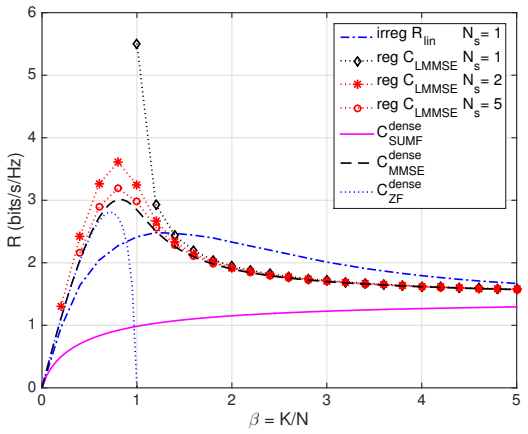

Fig. 6: Achievable rates (bits/s/Hz) of dense NOMA ($N_s = N$) with SUMF, MMSE, ZF receivers vs. low-dense NOMA ($N_s = 1, 2, 5$) with linear receivers as a function of β for fixed $E_b/N_0 = 10$ [dB]

NOMA ($2 \leq N_s \in \mathbb{N}^+, \beta N_s \in \mathbb{N}^+$) [11]. For any value of load, low-dense NOMA cases were shown to be more spectral-efficient than dense ones. For optimum receivers, achievable rates of the *regular* low-dense are higher than the *irregular* low-dense and dense NOMA regardless of load. To this end, the system must be constrained to have exactly N_s REs per user and $\beta N_s \in \mathbb{N}$ users per resource; this imposes either central scheduling or users coordination. For linear receivers, spectral efficiency of *regular* low-dense NOMA was proved to be higher than all the other cases in the underloaded regime, while spectral efficiency of *irregular* low-dense dominated other NOMA cases in the overloaded systems, particularly when the system load β is within an interval that is about [1.2, 5]. When N_s increases, that is sparseness decreases, achievable rates of low-dense cases rapidly converged to achievable rates of the dense case, as soon as $N_s = 2$.

In conclusion, by changing the spreading strategy from dense to low-dense, specific theoretical limits hold, showing that, to obtain higher achievable rates for linear decoders while still enjoying the lower receiver complexity, it is advisable to adopt sparse communications, and in particular *irregular* extreme low-dense schemes when systems are overloaded and *regular* extreme low-dense cases in the underloaded regime.

5 Acknowledgement

The authors would like to express their gratitude to Dr. Benjamin M. Zaidel for his fruitful comments and useful discussions regarding the regular low-dense NOMA case.

6 References

1 Ding, Z., Lei, X., Karagiannidis G. K., et al.: 'A survey on non-orthogonal multiple access for 5G networks: Research challenges and future trends'. IEEE J. on Sel. Areas in Commun., 2017, 35, (10), pp. 2181-2195
2 3GPP Portal, https://portal.3gpp.org/, accessed on 20 June 2018
3 Lien, S. Y., Shieh, S. L., Huang, Y., et al.: '5G New Radio: Waveform, Frame Structure, Multiple Access, and Initial Access'. IEEE Commun. Mag., 2017, 55, (6), pp. 64-71
4 Dai, L., Wang, B., Yuan,. Y, et al.: 'Non-orthogonal multiple access for 5G: solutions, challenges, opportunities, and future research trends'. IEEE Commun. Mag., 2015, 53, (9), pp. 74-81
5 Learned, R. E., Willsky, A. S., Boroson, D.M.: 'Low complexity optimal joint detection for oversaturated multiple access communications'. IEEE Trans. on Signal Process., 1997, 45, (1), pp. 113-123
6 Andrews, J.G.: 'Interference cancellation for cellular systems: a contemporary overview', IEEE Wireless Commun., 2005,12, (2), pp.19-29
7 Ding, Z., Liu, Y., Choi, J., et al.: 'Application of non-orthogonal multiple access in LTE and 5G networks', IEEE Commun. Mag., 2017, 55, (2), pp. 185-191
8 Shamai, S., Verdú, S.: 'The impact of frequency-flat fading on the spectral efficiency of CDMA', IEEE Trans. on Inf. Theory, 2001, 47, (4), pp. 1302-1327

Table 2 Properties of low-dense code-domain NOMA schemes

Multiple Access schemes	**LDS-CDMA/TH-CDMA**	**SAMA**	**MUSA**	**PDMA**
Based-domain	Sequence-based	Sequence-based	Sequence-based	Pattern-based
Entries of matrix $\boldsymbol{S}$	$\{+1, 0, -1\}$	$\{0, 1\}$	$\{1+i, -1+i, -1-i, 1-i\}$	$\{0, 1\}$ or $\{0, \alpha e^{-j\phi_{ki}}\}$
Relationship with other MA schemes	DS-CDMA with low-dense spreading sequences	LDS-CDMA with specific design of $\boldsymbol{S} \in \mathbb{R}^{N\times(2^N-1)}$	LDS-CDMA with grant-free access	LDS-CDMA with non-orthogonal patterns

9 Raymond, J., Saad., D.: 'Sparsely spread CDMA: a statistical mechanics-based analysis', Journal of physics, mathematical and theoretical, 2007, 40, (41), pp. 12315-12333

10 Shental, O., Zaidel, B. M., Shamai, S.: ' Low-density code-domain NOMA: Better be regular'. Proc. IEEE Int. Symp. on Inf. Theory (ISIT), July 2017, pp.2628-2632

11 Zaidel, B. M., Shental, O., Shamai, S.: 'Sparse NOMA: A Closed-Form Characterization', Proc. IEEE Int. Symp. Inf. Theory (ISIT), Vail, CO, USA, Jun. 17-23, 2018, pp. 1106-1110.

12 Ferrante, G. C., Di Benedetto, M.-G.: 'Spectral efficiency of random time-hopping CDMA', IEEE Trans. Inf. Theory, 2015, 61, (12), pp. 6643-6662

13 Le, M. T. P., Ferrante, G. C., Quek, T. Q. S., Di Benedetto, M.-G.: 'Fundamental Limits of Low-Density Spreading NOMA with Fading', IEEE Trans. Wireless Commun., 2018.

14 Li, K., Wang, X., Ping, L.: 'Analysis and optimization of interleave-division multiple-access communication systems', IEEE Trans. on Wireless Commun., 2007, 6, (5), pp. 1973-1982

15 Ping, L., Liu, L., Wu, K., Leung, W. K.: 'Interleave division multiple-access'. IEEE Trans. on Wireless Commun., 2006, 5, (4), pp.938-947

16 Hoshyar, R., Wathan, F. P., Tafazolli, R.: 'Novel low-density signature for synchronous CDMA systems over AWGN channel', IEEE Trans. on Signal Process., 2008, 56, (4), pp. 1616-1626

17 Dai, X., Chen, S., Sun, S., et al.: 'Successive interference cancelation amenable multiple access (SAMA) for future wireless communications'. Proc. IEEE Int. Conf. Commun. (ICC), Macau, China, Nov. 2014, pp. 222-226

18 Yuan, Z., Yu, G., Li, W., et al.: 'Multi-usershared access for internet of things'. Proc. IEEE Veh. Technol. Conf. (VTC- Spring), Nanjing, May 2016, pp. 1-5

19 Chen, S., Ren, B., Gao, Q., et al.:'Pattern Division Multiple Access- A Novel Nonorthogonal Multiple Access for Fifth- Generation Radio Networks', IEEE Trans. Veh. Technol., 2017, 66, (4), pp. 3185-3196

20 Zeng, J., Li, B., Su, X., et al.,:'Pattern division multiple access (PDMA) for cellular future radio access'. Proc. IEEE Wireless Commun. & Signal Process.(WCSP), Nanjing, China, 2015, pp. 1-5

21 Verdú, S., Shamai, S.: 'Spectral efficiency of CDMA with random spreading', IEEE Trans. Inf. Theory, 1999, 45, (2). pp 622-640

22 Al-Imari, M., Imran, M. A. , Xiao, P.: 'Radio Resource Allocation for Multicarrier Low-Density-Spreading Multiple Access'. IEEE Trans. on Veh. Tech., 2017, 66, (3), pp. 2382-2393

23 Nikopour, H., Baligh, H.: 'Sparse code multiple access', Proc. IEEE Annu. Int. Symp. Personal, Indoor, and Mobile Radio Commun. (PIMRC), London, UK, Sept. 2013, pp. 332-336

24 Moltafet, M., Mokari, N., Javan, M.R., et al.: 'A New Multiple Access Technique for 5G: Power Domain Sparse Code Multiple Access (PSMA)'. IEEE Access, 2018, 6, pp.747-759

25 Tulino, A. M., Li, L., Verdú S.: 'Spectral efficiency of multicarrier CDMA', IEEE Trans. on Inf. Theory, 2005, 51, (2), pp.479-505

26 Qin, Z., Yue, X., Liu, Y., et al.: 'User Association and Resource Allocation in Unified Non-Orthogonal Multiple Access Enabled Heterogeneous Ultra Dense Networks', IEEE Communication Magazine; accept to appear, arXiv preprint:1801.08198

27 Montanari, A., Tse, D.: 'Analysis of belief propagation for non-linear problems: The example of CDMA (or: How to prove Tanaka's formula)'. Proc. IEEE Inf. Theory Workshop, Punta del Este, Uruguay, Mar. 2006, pp. 160-164

28 Yoshida, M., Tanaka, T.: 'Analysis of Sparsely-Spread CDMA via Statistical Mechanics'. Proc. IEEE Int. Symp. on Inf. Theory (ISIT), July 2006, pp.2378-2382

29 Guo, D., Wang., C.: 'Multiuser detection of sparsely spread CDMA', IEEE J. on Sel. Areas in Commun., 2008, 26, (3), pp. 421-431

30 Benjamin M. Zaidel. Personal communications, 2018.

7 Appendix

Table 2 provides an overview on the different low-dense NOMA schemes, which are described in Sec. 2, with respect to the based-domain, entries of matrix $\boldsymbol{S}$, and how they are related to other multiple access schemes, particularly with the LDS-CDMA/TH-CDMA scheme.